Cetane number	-	38	55	D 613
Density (at 15˚C)	g/cm^3	0.921	0.883	D1298
Flash point	˚C	228	147	D93
Cloud point	˚C	2	-1	D93
Kinematic viscosity (at 40˚C)	mm^2/s	39	5.83	D445

4.10. Conclusions

Biodiesel was produced in laboratory by an economically viable transesterification reaction using a novel heterogeneous basic catalyst. The perovskite barium cerate was successfully prepared by sol-gel polymer precursor method. The desired structure was proved by PXRD, SEM, and FT-IR. Various Ba/Ce stoichiometric ratios were inspected for catalytic activity. Among all, perovskite barium cerate ($BaCeO_3$) was proved to be an active and stable catalyst for the methanolysis of karanja oil. The surface area analysis of $BaCeO_3$ was determined and its specific surface area (S_{BET}) was found to be $32m^2/g$, and its pore size distribution confirmed it as mesoporous material. The influence of various parameters such as catalyst dose, oil to alcohol molar ratio, reaction temperature, reaction time and agitation speed were thoroughly studied and the KOME with remarkable (98.4±0.4%) conversion was synthesized at optimum reaction conditions (catalyst dose;1.2 wt %, oil to methanol molar ratio;1:19, reaction temperature; 65˚C, reaction time;100 min, and agitation speed; 600 rpm. The reaction followed pseudo-first order kinetics. The activation energy (E_a) was 42.77kJ mol^{-1} and the frequency factor (A) to be $11.94\times10^4 min^{-1}$. Barium cerate has got the excellent reusability till sixth cycle with KOME conversion capacity greater than 81%. In present study, green chemistry metrics such as E-factor value of 0.088 illustrated $BaCeO_3$ catalysed transesterification reaction as a clean

production technique. TOF was also quantified as $21\times10^{-2}s^{-1}$ classifying the perovskite $BaCeO_3$ as efficient and sustainable catalyst for transesterification to produce biodiesel. The prepared KOME with the highest KOME conversion underwent for physicochemical analysis to assure its suitability for engines without modification. All the physicochemical properties accounted in this study were well within the permissible range prescribed by ASTM standards which approved the produced biodiesel a clean and efficient alternative for conventional diesel fuel.

CHAPTER-5

5.1. Introduction

In this chapter, Sr-La mixed metal oxide, novel solid heterogeneous base catalyst was emphasized for FAME production from *Schleichera oleosa* oil. The catalyst was characterized by XRD, XPS, FT-IR, SEM, EDX and BET surface area analysis alongwith basic strength determination. Effect of various factors including calcination time, temperature, reaction time, molar ratio (methanol: oil), and catalyst concentration were also taken into considered for optimization to obtain highest methyl ester conversion from *Schleichera oleosa* oil. Optimization of transesterification reaction was carried out via OVAT (one variable at a time) method. The confirmatory experiments noticed the highest (96.4±0.3 %) FAME conversion at following reaction conditions: catalyst dose (1.5 wt %), methanol to oil molar ratio (14:1), reaction temperature (65˚C), and reaction time (40 min). The pseudo-first order kinetic model was also successfully established the transesterification reaction having activation energy (E_a) of 65.26 kJ/mol to be a first order kinetics. Furthermore, thermodynamics was also explored and important thermodynamic functions (ΔH°, ΔS°, and ΔG°) were evaluated using Eyring equation. The Environment-factor (E-factor) and turn over frequency (TOF) were enumerated as 0.091 and $24\times10^{-2}s^{-1}$. The physicochemical properties of the synthesized methyl esters were measured according to ASTM D 6751 and were found to be within the permissible range.

5.2. Catalyst synthesis

Co-precipitation route was followed for the synthesis of Strontium Lanthanum oxide. For catalyst preparation, nitrate precursors of strontium and lanthanum were

taken in a definite stoichiometric ratio (Sr/La with molar ratio of 1:2) in distilled water. Mixed metal hydroxides were precipitated by dropwise addition of sodium carbonate solution at stirring speed of 600 rpm till a final pH of 12.5 was attained. The precipitated material was separated from its mother liquor using Whatman filter paper followed by drying in an oven at 80˚C overnight. Uncalcined material was examined through TGA/DTA. From thermal analysis, stable phase of the catalyst was obtained at 900˚C.Therefore, mixed metal hydroxide powder was calcined in a muffle furnace at 900˚C for 4h with a heating rate of 10˚C/min. Synthesized sample was ground with the help of agate mortar and sieved to obtain fine powder before it was used as a catalyst.

5.3. Catalyst characterization

5.3.1. Thermal analysis

The thermal behavior of the uncalcined catalyst was analyzed through TGA/DTA/DTG curve and has been shown in Figure 5.1.

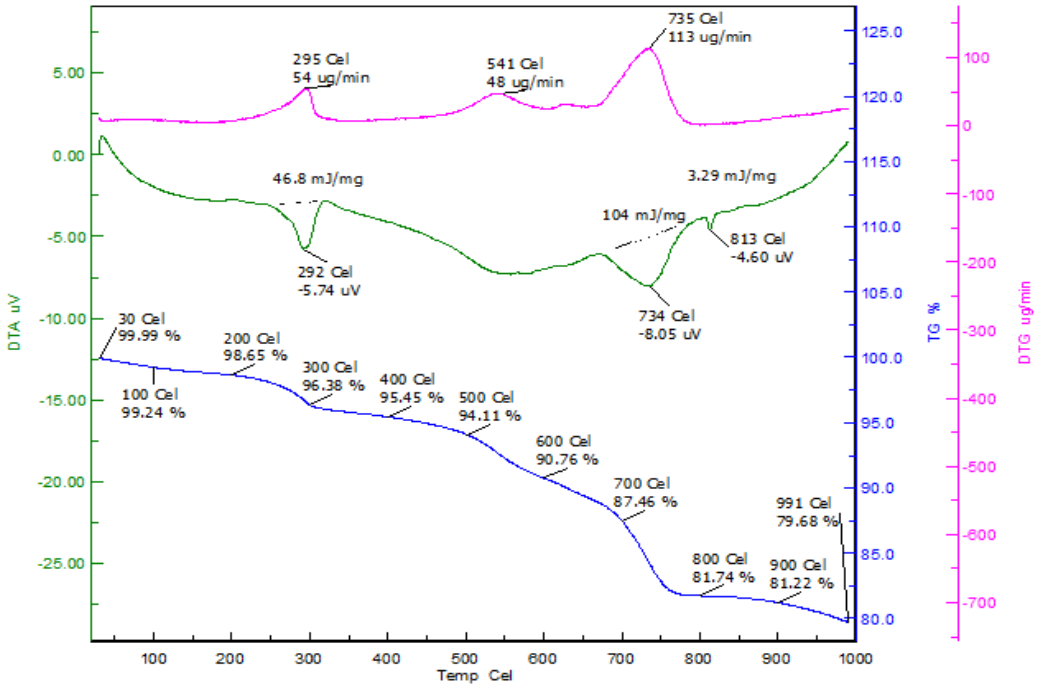

Figure 5.1 TGA /DTA/DTG curves of uncalcined catalyst.

Figure 5.1 contains thermo gravimetric (TGA) profile along with differential thermal analysis (DTA) and derivative thermo gravimetric (DTG) analysis which indicates three stages of weight loss. The temperature range of calcination started from ambient temperature to 1100˚C. The very first weight loss (2.27%), in the temperature range of 200-300˚C was caused by an endothermic event regarding to the loss of loosely absorbed water and water of crystalinity from prepared catalyst. The second weight loss of 3.35% was attributed to removal of co-precipitated nitrate over a broad temperature range of 450-680˚C. The major weight loss (5.72%) is regarded to the evolution of CO_2 from catalyst resulted through the degradation of trapped CO_3^{2-}. According to DTA, all three weight loss processes are found to be endothermic in nature. Onward 850˚C, there is no further considerable weight loss, which further indicates that material achieved required phase stability.

5.3.2. Powder XRD analysis

X-ray diffraction (XRD) is extensively used analytical technique for phase identification of crystalline compounds along with unit cell parameters. In X-Ray diffractogram, crystalline material attributes to sharp peaks with relatively higher intensity. The peaks in Figure 5.2 are quite sharp, which further confirm the crystallinity of the synthesized catalyst. It can also be seen from Figure 5.2 (a, b, c, & d) that prominent peaks get more intensified with increase in calcinations time duration, hence more crystalline catalyst is obtained. The prominent peaks were matched with the JCPDS file (no 72-0893).In Figure 5.2(a), only 6 major peaks with mild intensities was observed but further increment in time duration, one more peak related to (400) was evolved which onward got intensified showing the proper phase formation of stable monoclinic crystal with unit cell parameter a (11.65), b (7.34), c(13.47), α(90˚),

β(115.60˚) and γ(90˚). From XRD, the empirical chemical formula of catalyst has been confirmed upon matching with aforementioned JCPDS file as $Sr_3La_4O_9$.

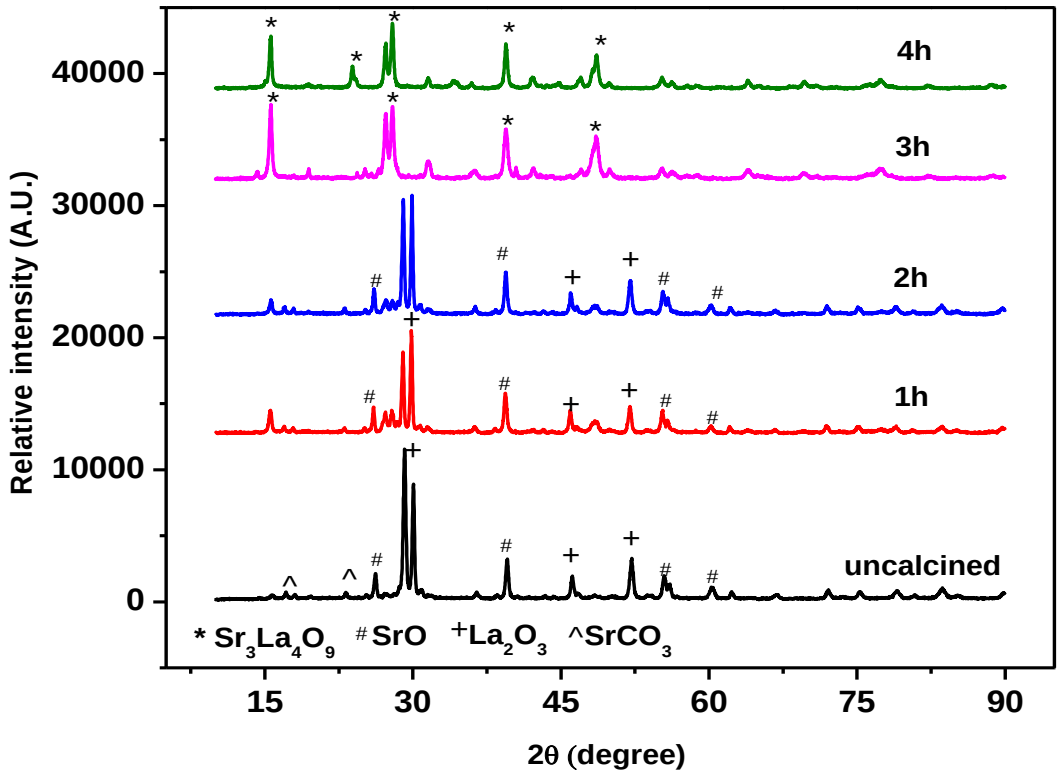

Figure 5.2 X-Ray diffractogram of calcined catalyst at 900˚C for 1 h (a), 2 h (b), 3 h (c) and 4 h (d).

5.3.3. Surface morphological analysis

SEM analysis of the catalyst was conducted to explore its surface morphologies along with EDS for elemental composition. SEM of the catalyst reveals that the particles are very irregular in shape. Figure 5.3 represents the micrograph of uncalcined catalyst as well as calcined catalyst at 900^0C for different time period. From Figure 5.3(a), it can be clearly observed that the uncalcined catalyst is in highly irregular and clustered form. Because of availability of less active surface, uncalcined material was not able to give high conversion efficiency. Onward extension in calcination time duration enabled particles to be separated and produced tiny entities as

in Figure 5.3 (b, c, &d). In Figure 5.3(e), crystals appeared as well dispersed entities. The particle size distribution analysis of the catalyst was carried out by means of Image J software using SEM micrograph. The particle size was found to be in the range of 0.5-3.5 µm (Figure 5.4). Energy Dispersive X-Ray spectroscopy (EDS) of the selected area of the catalyst was conducted and the result (Figure 5.5) confirmed presence of strontium lanthanum mixed metal oxide in an appropriate stoichiometry. Figure 5.5 illustrated that mixed metal oxide contains lanthanum (16.95%), strontium (18.50%) and oxygen (64.56%).

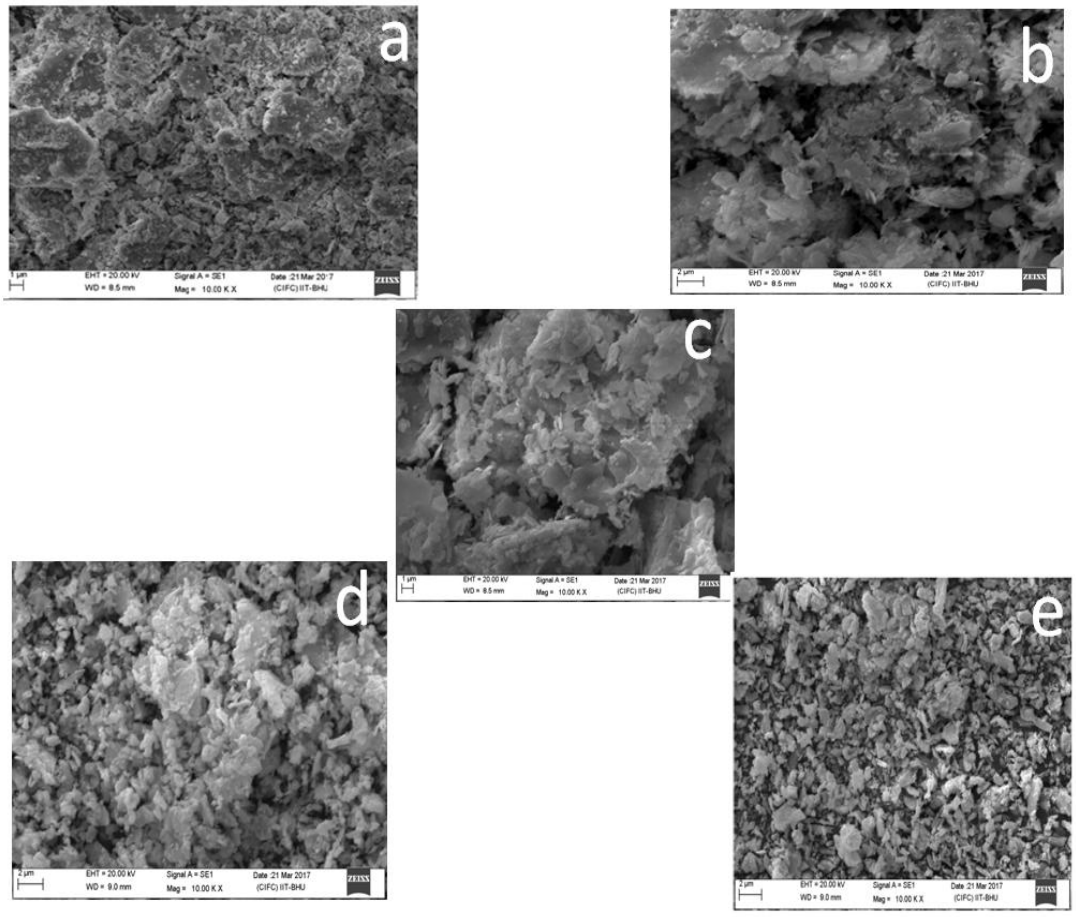

Figure 5.3 SEM images of (a) uncalcined catalyst and calcined catalyst at 900˚C for (b) 1 h, (c) 2 h, (d) 3 h, and (e) 4 h.

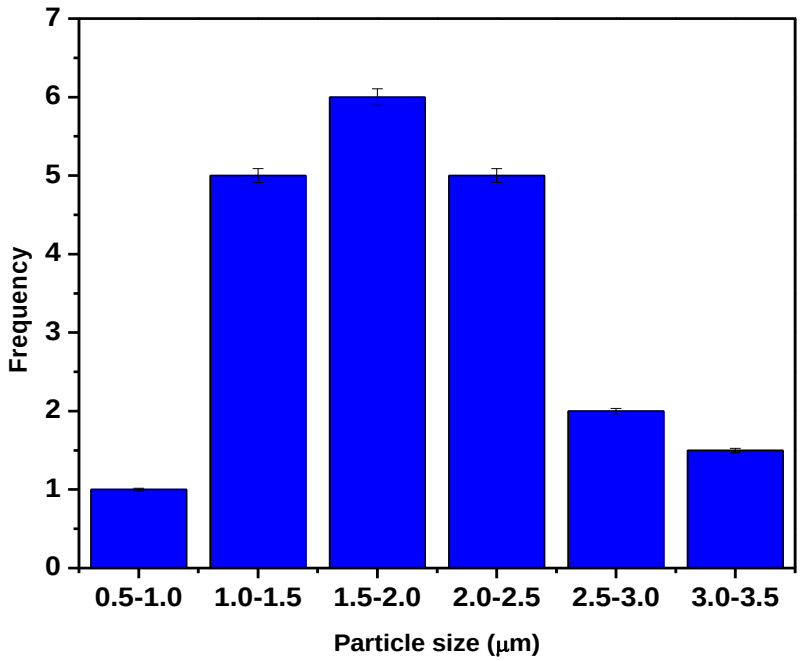

Figure 5.4 Particle size distribution of the catalyst using SEM image.

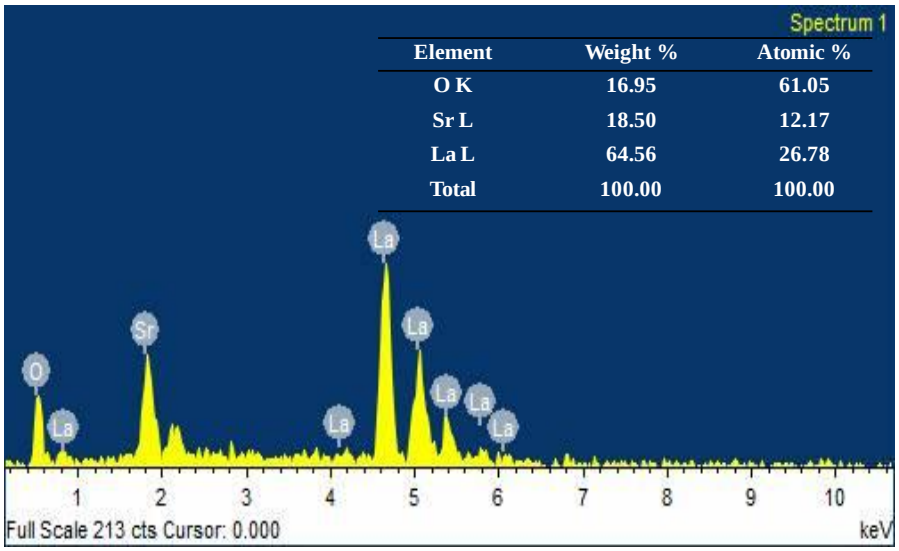

Figure 5.5 EDXS histogram of calcined catalyst at 900˚C for 4h.

5.3.4. BET surface area analysis

Figure 5.6(a) depicted N_2 adsorption-desorption curve with characteristic hysteresis loop reflecting the mesoporous nature of the material. The BET surface area

and average pore size of prepared catalyst was found to be 15.9 m^2/g and 2.21nm respectively. The pore volume of the catalyst was measured and found to be 0.035cm^3/g. The pore diameter of the synthesized catalyst was found to be in the range of 1.5-60 nm (i.e. characteristics of mesoporous material) (Figure 5.6(b)) which was comparable with the size of triglyceride molecule (size ~ 6 nm) (Sahani and Sharma, 2018).

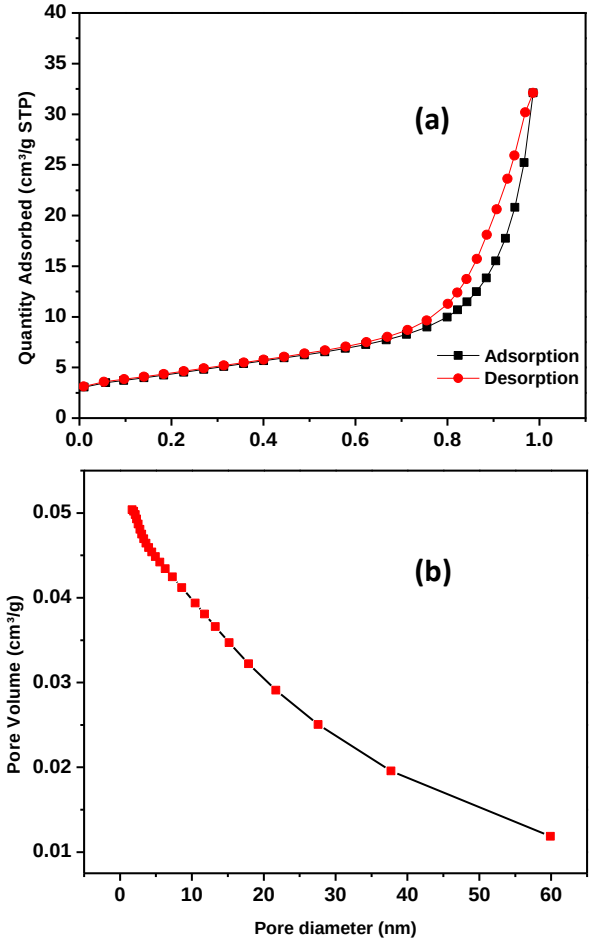

Figure 5.6 (a) N_2 adsorption-desorption profile of the catalyst; (b)BJH adsorption pore size distribution of the catalyst.

However, from the pore size analysis average pore size diameter was obtained as 2.21nm, which further indicated that porosity factor had limited contribution in the

transesterification process, as the triglyceride molecule remain inaccessible to the interior part of the catalyst surface. Thus, the observed interaction supposed to be taken place on the catalyst's external surface.

5.3.5. XPS analysis

Figure 5.7(a) show the X-Ray photoelectron spectrum of prepared catalyst showing characteristic elemental peaks of Sr, La and O. Figure 5.7(b) represents the Sr 3d line in the mixed metal oxide calcined at 900˚C for 4 h with highest catalytic activity. It consists of a doublet peak at 131.86 eV and 133.56 eV corresponding to Sr $3d_{5/2}$ and Sr $3d_{3/2}$ respectively. This attributes to presence of Sr^{2+} in mixed metal oxide. It is observed that Sr $3d_{5/2}$ is found to be shifted from its theoretical value by 1 eV probably due to mixed metal oxide formation. The identical peak patterns are also validated by Hinnen et al. (1995). Figure 5.7(c) shows the peaks pattern of La^{3+} in mixed metal oxide. The characteristic peak of La ion regarding La 3d state is split into La $3d_{3/2}$ and La $3d_{5/2}$ due to spin-orbit interaction owing to charge transfer from higher energy filled orbital of oxygen to vacant La 4f. The main characteristic line corresponding to La $3d_{5/2}$ is found to be at~ 834eV and energy difference between La $3d_{3/2}$ and La $3d_{5/2}$ is 19eV. Further, these results are supported by Wu et al., (2005). Figure 5.7(d) represents the main peak regarding O (1s) at 529.5eV which ultimately confirms its oxide state in the prepared catalyst.

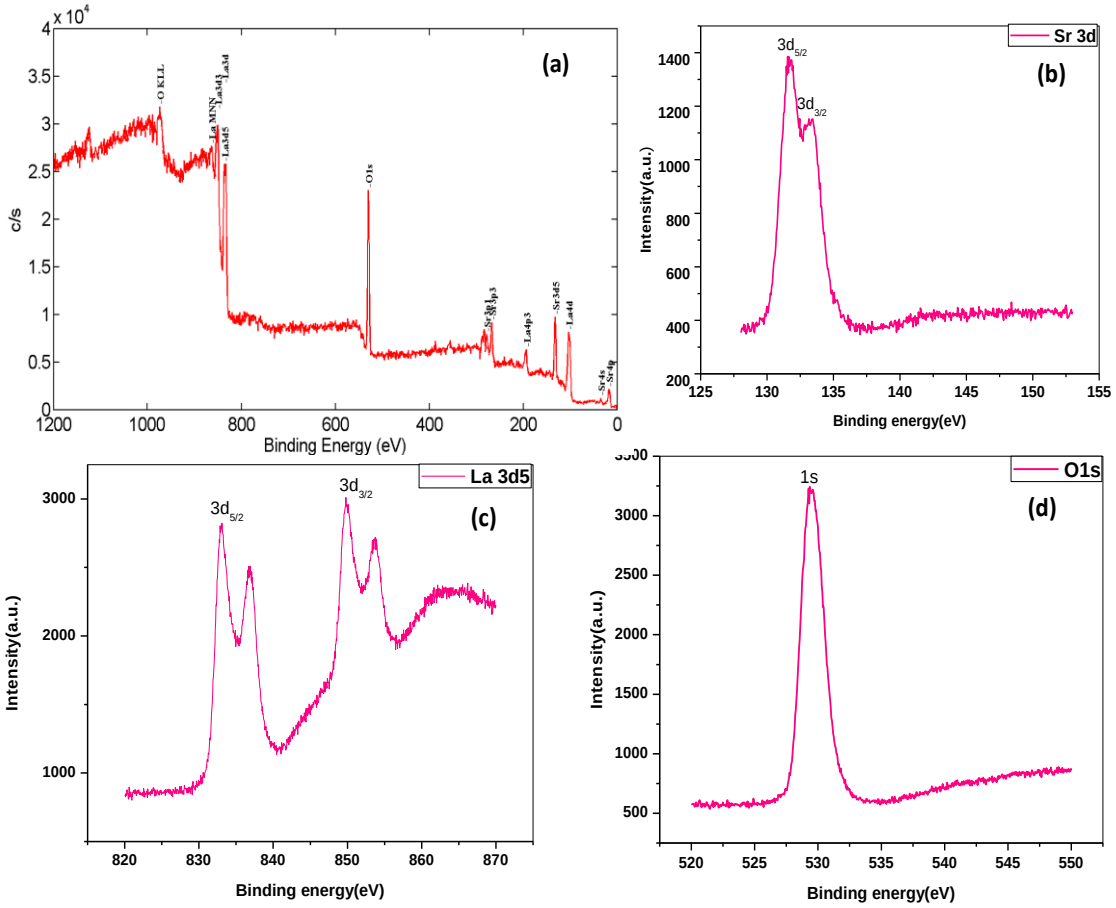

Figure 5.7 X-Ray photoelectron spectra of the synthesized catalyst (a) Sr XPS 3d spectra (b) La XPS 3d spectra. (c) O XPS 1s spectra of strontium lanthanum mixed metal oxide.

5.3.6. FT-IR analysis

FT-IR analysis was executed to explore the functional groups present in synthesized catalyst Figure 5.8(a-d) depict FT-IR spectra of fresh catalyst calcined at 900˚C for 4 h. It also provides the information regarding surface poisoning after transesterification reaction which cannot be correctly interpreted by XRD. Figure 5.8 demonstrates the FT-IR spectra of synthesized catalyst calcined at each one hour time interval i.e. 1 h, 2 h, 3 h and 4 h. In each individual spectrum, number of peaks as well as their positions are almost same except the peak broadening. From FT-IR spectra, peak corresponding to M-O bond is sharpened as calcination time increases from 1 h to

4 h. Further, peaks corresponding to O-H and C=O stretching become insignificant with increment in calcination time. In Figure 5.8(d), peak belonging to M-O bond is very sharp with insignificant impurities. The peak observed at 3610 cm^{-1} attributed to O-H vibration of H_2O as well as free O-H group on surface of catalyst. Another vibration peak at 2350cm^{-1} corresponds to adsorbed atmospheric CO_2 on the surface . A low intensity peak at~1636cm^{-1} ascribed to bending mode of vibration in water molecule. The prominent peaks at 845 and 603cm^{-1} are due to stretching vibrations of metal oxygen bonds (Sr-O and La-O).

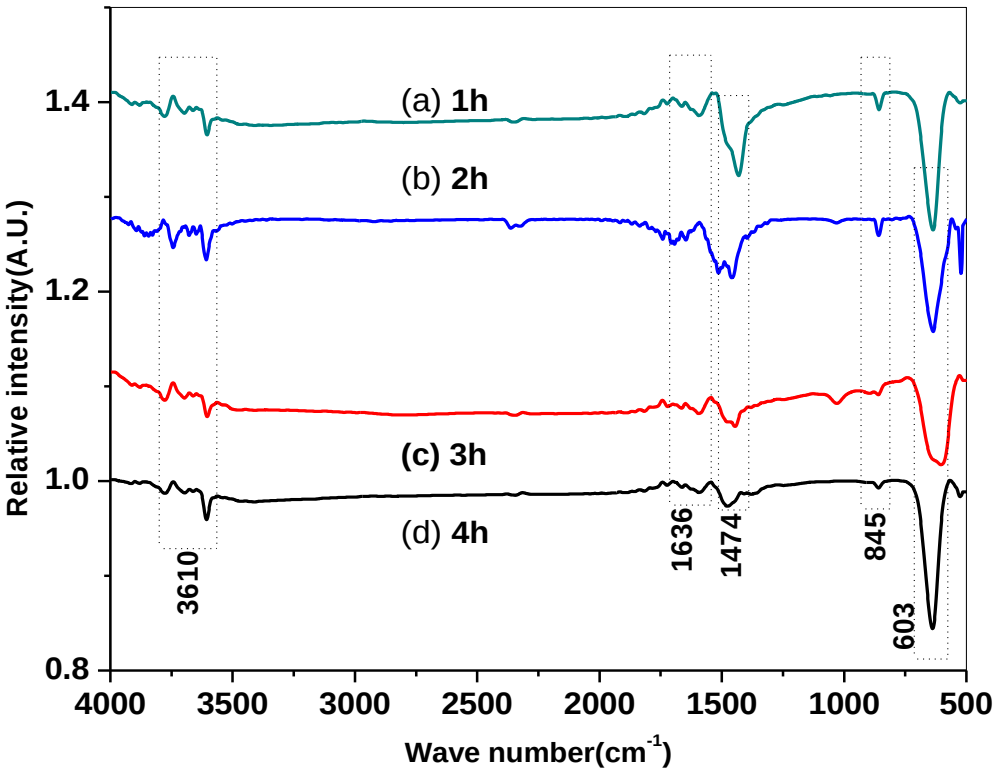

Figure 5.8 FT-IR spectra of calcined catalyst at different calcination time intervals.

5.3.7. Basicity

Charge density residing on M-O bond offers the Lewis basicity which generates the acyl acceptor by polarizing the O-H bond in alcohol used for transesterification

reaction. The Lewis basicity of strontium lanthanum oxide was determined using Hammett indicator-benzoic acid titration method. Total basicity of mixed metal oxide was found to be 2.77mmol/g.

5.4. Effect of process variables on FAME conversion

In present study, impact of various process variables viz. calcinations time duration, presence of co solvent, catalyst concentration, oil-to-methanol molar ratio, reaction time, reaction temperature and stirrer speed on the FAME conversion were inspected. In optimization process, the catalyst concentration was studied in the range of 0.5-2.5wt%. Oil-to-methanol molar ratio was varied from 1:5 to 1:20. Co-solvent concentration was kept proportionate to methanol in 1:1 ratio. Among all co-solvents, di-isopropyl ether (DPE) was found to be most effective, and it is attributed to its capacity to stabilize the polar material (methanol) in mixture via hydrogen bonding along with alkyl group which can easily be mixed up in oil phase. Reaction time was varied from 20 to 120 min; reaction temperature, 40˚C to 90˚C; and stirrer speed, 300 to 800 rpm.

5.4.1. Effect of calcination time

The effect of calcination time on the activity of Strontium Lanthanum oxide was examined by performing the transesterification reactions of *Schleichera Oleosa* oil for biodiesel production keeping all other process variables constant. Calcination time plays a noteworthy role in active catalyst formation which has higher number of active sites as well as higher surface area without agglomeration at elevated temperature. Figure 5.9(a**)** shows that calcination of the synthesized catalyst at 900˚C for 1h, 2h, and 3h respectively, was not sufficient in terms of catalytic activity for FAME conversion.

The synthesized catalyst calcined at 900˚C for 4h showed better transesterification activity with 90% FAME conversion at reaction conditions molar ratio of 1:17 (oil: methanol), 2 wt% of catalyst dose at 65˚C for 1 h with 500 rpm.

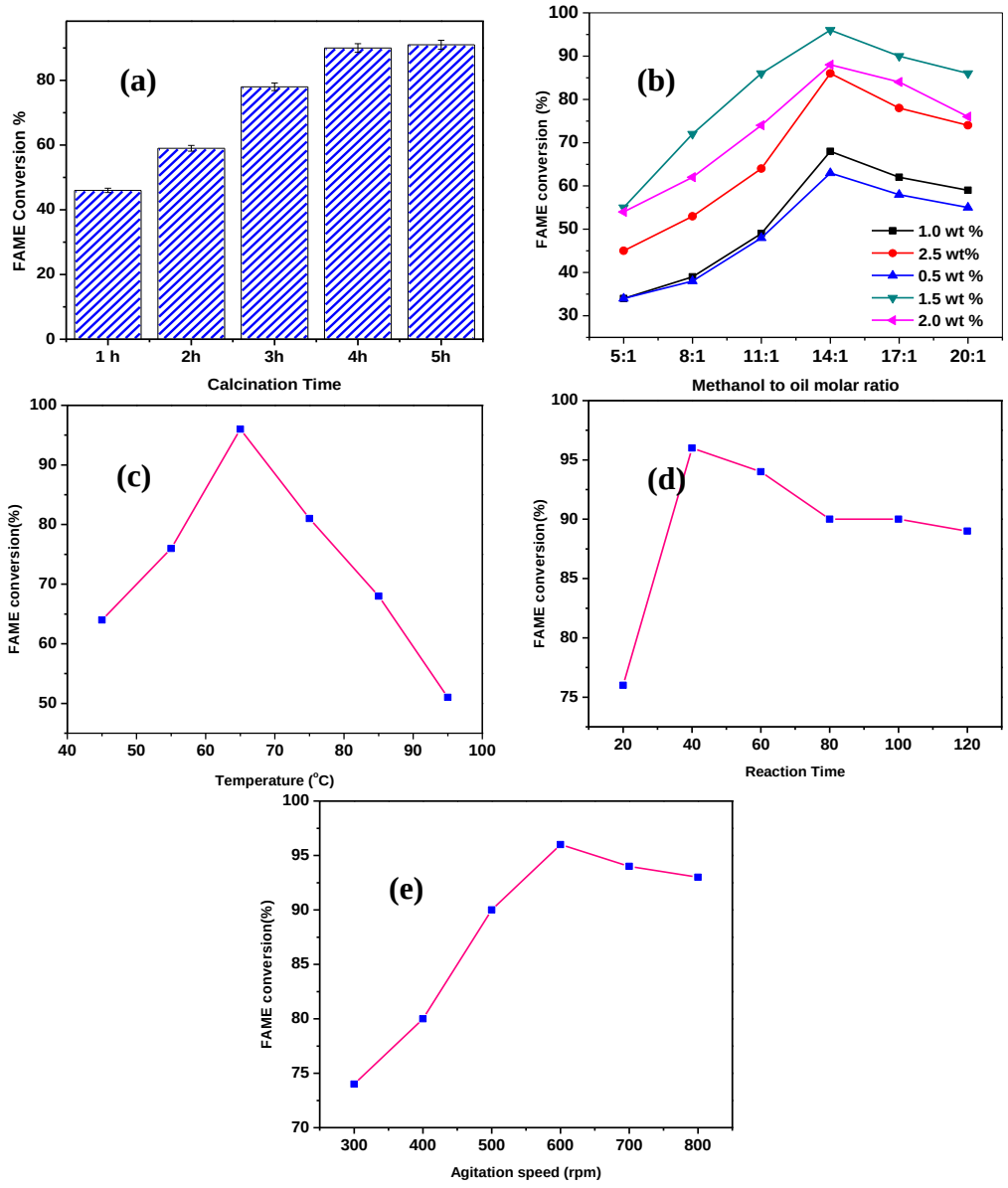

Figure 5.9 An illustration of effect of (a) calcination time duration, (b) catalyst dose and methanol to oil molar ratio, (c) reaction temperature, (d) reaction time, (e) agitation speed on FAME conversion.

Moreover, the XRD results obtained at different time interval demonstrated that product calcined up to maximum time period of 4h results in the formation of catalyst

having high degree of crystallinity. This finding further supports the results obtained for maximum FAME conversion (90%) by using catalyst with highest catalytic activity calcined for 4h. However, further increment in calcination time does not result in any significant rise in FAME conversion. Therefore, making process less energy intensive, catalyst calcined at 900˚C for 4h was chosen for further optimization of the other process variables for maximum FAME conversion. This is due to calcination at 900˚C for 4 h led to complete formation of catalytically active stable mixed metal oxide from its precursors after desorption of CO_2 from catalyst.

5.4.2. Effect of methanol to oil molar ratio and catalyst dose

Methanol to oil molar ratio is one of the most significant parameters affecting FAME conversion as well as biodiesel production cost. Vyas et al, (2011) reported that alcohol to oil molar ratio significantly influenced the transesterification process. Theoretically, stoichiometric reaction requires only 3:1 alcohol to oil molar ratio. Due to reversible nature of transesterification reaction, higher alcohol to oil molar ratios than aforementioned stoichiometric ratio must be provided to shift the reaction in forward direction as well as to enhance the contact between the alcohol molecule and the triglycerides. In case of non-edible feedstock, comparatively more alcohol is desired to reduce viscosity of reaction mixture. Besides, catalyst too plays a major role to facilitate the reaction by providing the new path of low activation energy as discussed above.

To determine the optimized values of methanol: oil molar ratio along with catalyst dose, several transesterification reactions were executed using alcohol to oil molar ratio varied from 5:1 -20:1 wt% with variation in catalyst dose from 0.5 -2.5 wt % for 1 h and at 65˚C with stirring speed of 500 rpm. Figure 5.9(b) shows the

combined effect of catalyst concentration and methanol:oil molar ratio on FAME conversion. From Figure 5.9(b), it can be clearly observed that there is significant increment in conversion (96%) of mono alkyl ester at optimum value of 1.5 wt % catalyst dose with 14:1 alcohol to oil molar ratio along with co-solvent. In absence of co-solvent, the same was found to be only 90% which does not fulfil the ASTM standard criterion. Further increment in catalyst concentration leads to higher viscosity of reaction mixture which ultimately retards methyl ester production as a result of limited mass transfer while higher alcohol to oil molar ratio starts assimilating glycerol which draws the reaction in backward direction and consequently lowers down the biodiesel formation and glycerol separation (Balat and Balat, 2010).

5.4.3. Effect of reaction temperature

The transesterification reaction of *Schleichera Oleosa* oil using 1.5wt% of catalyst was processed at 40˚C to 90˚C temperature range with oil to methanol ratio of 1:14, 60 min reaction time at 500 rpm. Figure 5.9(c) presents effect of temperature on methyl ester conversion with addition of the co-solvent. From Figure 5.9(c), it can be clearly seen that ester conversion increases with rise in temperature from 40˚C up to 65 ˚C. The optimum temperature was found to be 65˚C in presence of co-solvent. As kinetic energy is the function of temperature of the system, the higher temperature corresponds to higher kinetic energy of reactant molecule. So higher temperature reduced the viscosity of reaction mixture and enhances methyl ester conversion. However, after reaching certain threshold value of temperature (boiling point of methanol: 64.7˚C) in reaction mixture, ester conversion started declining because of evaporation of methanol, thus reducing the contact between methanol and triglyceride.

5.4.4. Effect of reaction time

Reaction time needed for completion of a transesterification relies on the extent of proper contact among reactant molecules. Optimization process was executed by varying the reaction time in the range of 20 to 120 min with a catalyst dose of 1.5 wt%, reaction temperature of 65°C, oil-to-methanol ratio of 1:14 and a stirrer speed of 500 rpm. Figure 5.9(d) shows the effect of reaction time on FAME conversion again in presence of co-solvent. From Figure 5.9(d), the mono alkyl ester conversion in presence of co-solvent was observed to attain the maximum (96%) within 40 min of contact time. Increasing reaction time beyond optimized value, formation of *Schleichera Oleosa* hydrolysate gradually deters the conversion efficiency. Hence, optimization of exact required reaction time is crucial for gaining maximum conversion. The optimum time required for transesterification reaction was obtained to be 40 min at 65˚C and 600 rpm in presence of co-solvent.

5.4.5. Effect of agitation speed

Proper mixing of reactants is critically important in transesterification reaction as reaction system is heterogeneous with three different phases. In present study, experiments were performed in presence of co-solvent by varying stirrer speed from 300 rpm to 800 rpm keeping other process parameters constant: oil-to-methanol ratio at 1:14, the catalyst dose at 1.5 wt%, and reaction temperature at 65˚C for optimized time interval with co-solvent (Figure 5.9(e)). Maximum conversion (96.37%) was observed at stirring speed of 600 rpm. Increment in the stirring speed beyond the optimum value results in no significant increase in conversion instead a slight decrease is observed due to vaporisation of methanol which ultimately reduces its contact with other reactant and catalyst. In each experiment, it was noted that the addition of co-solvent resulted a

higher FAME conversion efficiency.

5.5. Kinetic and thermodynamic studies

The kinetic plot in Figure 5.10(a) exhibits the rational linearity anticipating the precision of the applied kinetic model of pseudo first order kinetics (Banerjee et al., 2019). Furthermore, the rate constants at temperatures 323 K, 328 K, 333 K and 338 K were determined and found to be 4.5×10^{-2} min^{-1}, 7.23×10^{-2} min^{-1}, 1.0×10^{-1} min^{-1} and 1.3×10^{-1} min^{-1} respectively. The experimentally derived rate constants support the outcome that higher temperature accelerates transesterification process owing to promoted mass transfer. The activation energy (E_a) and pre-frequency factor (A) are calculated to be 65.264 KJ/mole and 15.8×10^{8} using Arrhenius plot in Figure 5.10(b). This observed value of activation energy derived on the basis of kinetic experiments was substantiated by previous reports in literature regarding biodiesel production using heterogeneous catalyst (Yadav et al., 2018). It further interpreted the chemical reaction occurring on the surface of catalyst as the rate determining step also validating the adopted kinetic model in current study. The investigation of thermodynamic functions in transesterification process was helpful in interpreting the mechanism involved in the process. Hence, from Eyring equation the value of ΔH° and ΔS° could be computed from the slope and intercept of the plot ln(k/T) versus 1/T respectively. Figure 5.10(c) depicted the Eyring-Polanyi profile for Sr-La mixed metal oxide catalyzed transesterification reaction. The thermodynamic functions (ΔH° and ΔS°) were evaluated as 62.511kJ/mol and -77.56J/mol respectively. The positive ΔH° value approved the transesterification reaction as endothermic in nature which further justified that external heat energy was critically needed to promote the reactants subsequent transformation into an activated complex**.** The negative ΔS° attributed to

rapid formation of reactant-catalyst complex that consequently reduced the randomness of the system. ΔG˚ values were estimated to be 87.56kJ/mol, 87.95 kJ/mol, 88.34 kJ/mol and 88.73 kJ/mol for the reaction temperature 50˚C, 55˚C, 60˚C and 65˚C, respectively. The positive ΔG˚ value indicated the non-spontaneous nature of the reaction in which transition state is having the higher energy level than reactants. Cumulatively, the positive values of ΔG˚ and ΔH˚ and negative value of ΔS˚ indicated the non-spontaneous and endergonic nature of the transesterification reaction (Roy et al., 2020).

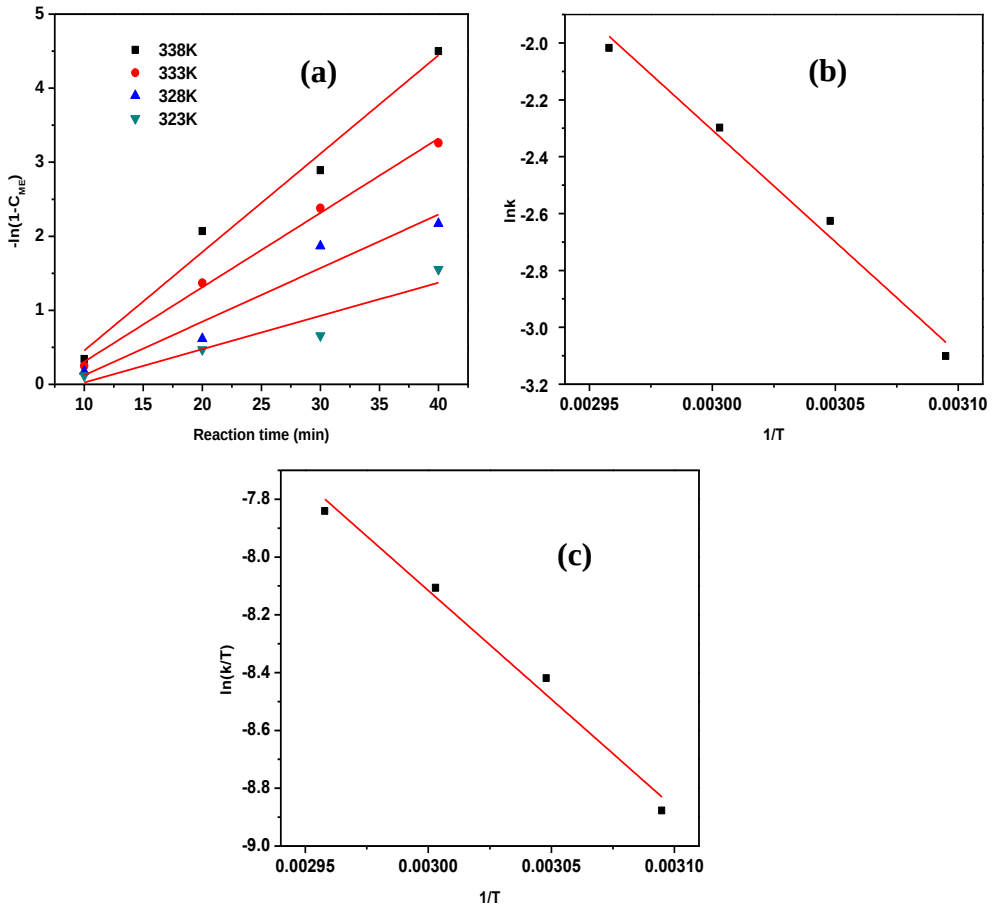

Figure 5.10 (a) -ln(1−C_{ME}) versus reaction time (min) plot for pseudo-first order kinetics, (b) Arrhenius plot,(c) Eyring plot.

5.6. Reusability test and leaching studies

Heterogeneous catalyst overcomes the problem of non-reusability associated with homogeneous catalyst as it can be easily separated once used. Experiments were performed by keeping all the process variables at their optimized values. For reusability, the catalyst was washed with hot methanol to eliminate organic impurities present on the catalyst surface. Thereafter, catalyst was dried in a hot air oven at 100˚C for 3h followed by calcination at 600˚C for 2 h. From Figure 5.11, it can be clearly observed that catalytic activity got decreased gradually up to the eight runs. To analyze the leaching property of the catalyst, SEM/EDXS was performed which substantiated that catalyst maintained its entity throughout the recycling process as no loss in stoichiometry was observed. It is also inferred from Figure 5.11 that the catalyst restores its functionality even after 8 runs with more than 75% FAME conversion. Thus, catalyst can be effectively employed for eight runs without severe loss of activity. It would be the basis for economically viable application of this catalyst which reduces the overall cost of transesterification reaction for biodiesel production.

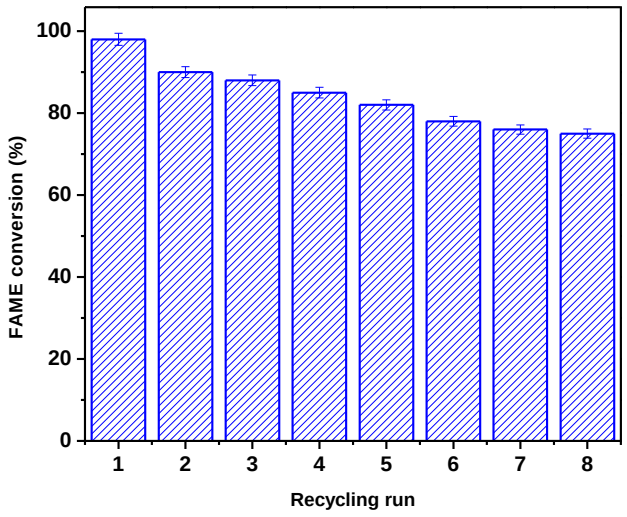

Figure 5.11 Catalyst reusability profile.

The gradual decrease in catalytic activity of employed catalyst was attributed to catalytic surface poisoning. FT-IR analysis has been carried out to comprehend the possible phenomenal interaction of organic moieties with the catalyst. From FT-IR spectra of both used and fresh catalyst, it can be predicted that the surface got covered with organic species, therefore, several peaks corresponding to C-H, C-C stretching as well as bending vibrations can be clearly seen in figure 15. It also broadened M-O stretching peak in the spectra. In Figure 5.12, sharp peaks with high intensity around 2850 cm^{-1} and 2985 cm^{-1} attributed to different C-H stretching ($-CH_2$, $-CH_3$) and –CHO respectively. The peaks around 1650 cm^{-1} are related to C=C stretching and –C=O bond residue present in fatty acids. Further, the peak adjacent to this around 1490 cm^{-1} corresponds to C-H bending vibration. This showed the catalytic poisoning of surface after multiple recycling.

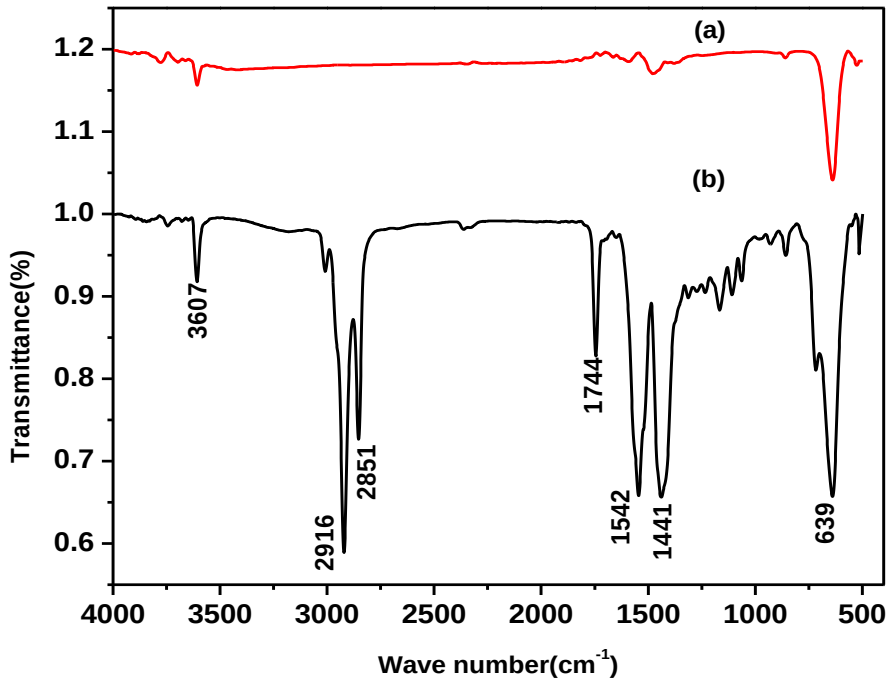

Figure 5.12 FT-IR spectra for comparative study of (a) fresh and (b) used catalyst.

5.7. E-factor and TOF

E-factor was calculated and found to be 0.091 which indicates that the heterogeneous basic catalysed transesterification reaction to have a green approach for a cleaner biodiesel production. TOF for KOME formation through transesterification reaction using $BaCeO_3$ was calculated to be 24×10^{-2} s^{-1}. The similar observations for TOF are also reported in literature (Umdu and Seker, 2012; Moura et al, 2016). The insignificant E-factor and appreciable TOF values propose the $BaCeO_3$ as a sustainable and potential solid catalyst for greener transesterification reaction.

5.8. Methyl ester characterization

5.8.1. GC-MS

Gas chromatogram of methyl esters derived from *Schleichera oleosa* oil was shown in Figure 5.13. Mass spectrum was interpreted by means of NIST database. The components present in the sample were identified and described in Table 5.1. As shown in chromatogram, there are three major peaks corresponding to three fatty acids i.e. eicosanoic acid, oleic acid, palmitic acid having retention time of 5.18 min, 5.74 min and 7.68 min, respectively. The oleic acid is found to be the major component in *Schleichera oleosa* oil derived methyl ester.

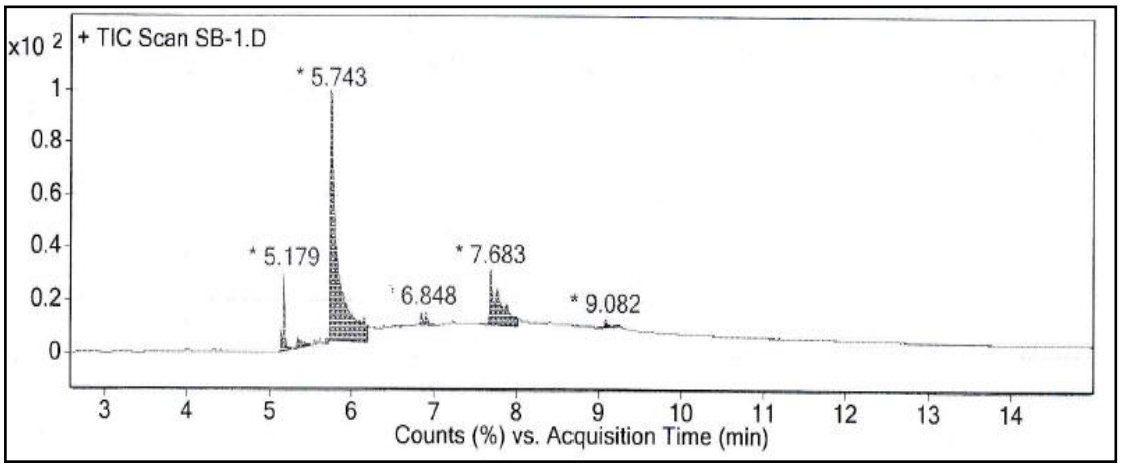

Figure 5.13 GC-MS profile of fatty acid methyl ester derived from *Schleichera oleosa* oil.

Table 5.1

Composition of *Schleichera oleosa* oil inferred from GC-MS

S.No.	Retention time (min)	Corresponding fatty acid	Area sum (%)
1	5.179	Eicosanoic acid	5.64
2	5.743	Oleic acid	69.86
3	6.848	Stearic acid	2.06
4	7.683	Palmitic acid	19.53
5	9.082	Linoleic acid	0.71

5.8.2. ^{1}H-NMR and ^{13}C-NMR

The fatty acid methyl ester from *Schleichera oleosa* oil was analyzed by ^{1}H-NMR spectroscopy shown in Figure 5.14(a). The characteristic signal attributed to methoxy protons in FAME appeared as a singlet at δ3.68 ppm. The triplet signal at δ 2.30 ppm was related of α-CH_2 protons of ester (Madhu et al., 2017). The quantification of methyl ester conversion was executed through ^{1}H-NMR analysis and 96.37% FAME conversion was achieved. Figure 5.14(b) illustrated the ^{13}C-NMR spectrum of fatty acid methyl ester from *Schleichera oleosa* oil. The signal of carbonyl carbon of methyl ester (-COOMe) in methyl ester emerged at 174.58ppm while methoxy carbon in FAME appeared at 51.69 ppm.

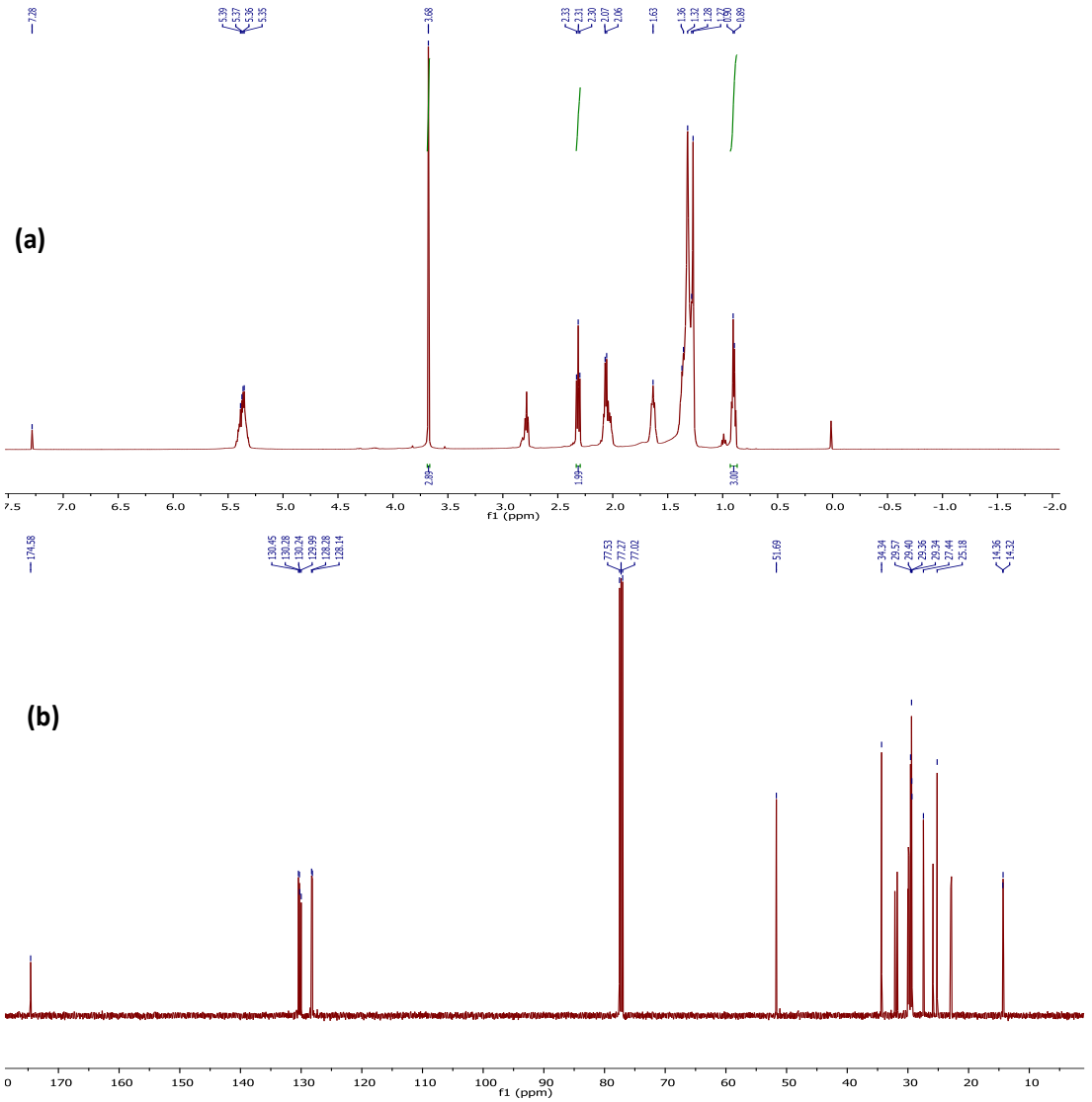

Figure 5.14 ^{1}H-NMR and ^{13}C-NMR spectra of synthesized methyl esters at optimized conditions of process variables.

5.8.3. ATR FT-IR

Figure 5.15 demonstrates ATR FT-IR spectra of synthesized fatty acid methyl ester from *Schleichera oleosa* oil. It contains all the characteristics peaks corresponding stretching vibrations of functional groups present in FAME with carbonyl stretching vibration in methoxy group at 1740 cm^{-1}.

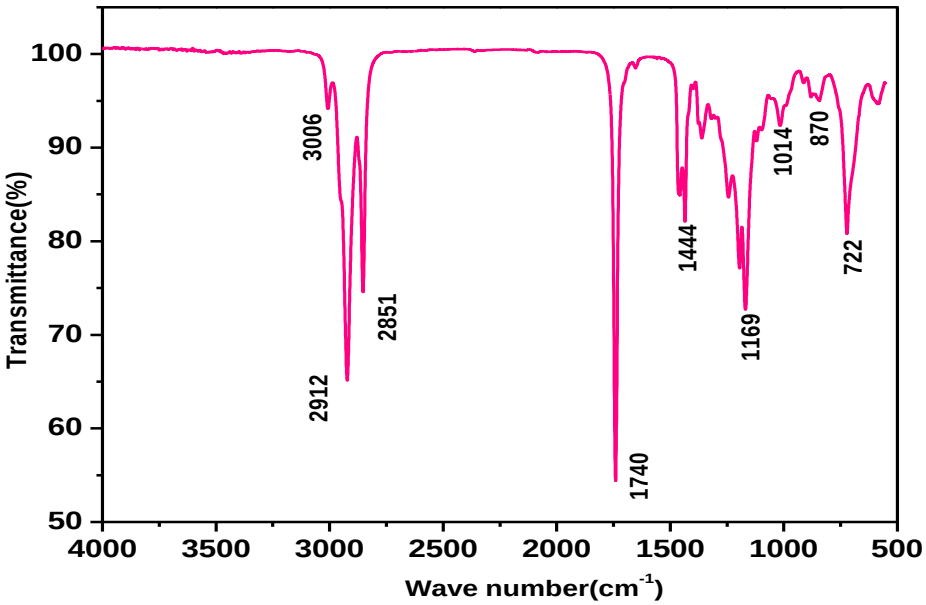

Figure 5.15 ATR FT-IR spectra of synthesized fatty acid methyl ester.

5.8.4. Investigation of physicochemical properties of methyl ester

Table 5.2 illustrated the comparative study of physicochemical properties between *Schleichera oleosa* oil and FAME. It can be clearly seen from the table that acid value was lowered down from 12.4 to 0.5 mg KOH/g. Kinematic viscosity has been reported to be drastically lowered down from 19 to 5.6 within prescribed ASTM standards. Relative density measurements of *Schleichera oleosa* oil as well as FAME were also performed. Flash point and fire point for both feedstock and biodiesel were also determined and were found to be within ASTM standards.

Moreover, the major important properties of a fuel such as cetane number and calorific value were found to be within ASTM standards. All above mentioned properties of produced biodiesel indicated its compatibility with CI engine.

Table 5.2

Comparative study of physicochemical properties of *Schleichera oleosa* oil and *Schleichera oleosa* oil methyl ester.

Properties	**Unit**	**Feedstock**	**FAME**	**ASTM Standards**
Acid Value	mg KOH/g	12.4	0.5	D664
Cloud Point	˚C	-	-4.2	D2500
Color	-	Yellowish red	Pale yellow	Yellowish
Calorific Value	(MJ/kg)	41.97	38.65	D4809
Cetane number	-	36	49.5	D613
Copper strip corrosion	-	1a	1a	D130
Density (at 15˚C)	g/cm^3	0.869	0.844	D1298
Flash Point	˚C	210	101	D93
Kinematic Viscosity(at 40˚C)	mm^2/s	19	5.6	D445
Fire Point	˚C	223	120	D93
Saponification value	mg KOH/g	182	173	D5558
Oxidative stability(at 110˚C)	-	14.4	7.9	EN14110

5.9. Conclusions

Biodiesel was synthesized from *Schleichera oleosa* oil by two step process i.e. esterification followed by transesterification reaction. A novel catalyst used in transesterification reaction was synthesized and characterized with various instrumentation techniques such as TGA/DTA/DTG, PXRD, SEM-EDX, XPS, FT-IR, and BET surface area analysis. Thermal analysis suggested that phase stability of the catalyst is achieved at 900˚C. XRD results indicated that catalyst attain high

crystallinity at 900˚C up to 4h of calcination. Surface area and average pore size of the catalyst estimated from the N_2 adsorption desorption isotherm as 15.9 m^2/g and 2.21 nm, respectively. FT-IR analysis confirmed the formation of mixed metal oxides. Free fatty acid composition of feedstock was examined by GC-MS analysis and oleic acid analyzed as major fatty acid component. Synthesized biodiesel was characterized by ^{1}H-NMR, ^{13}C-NMR, FT-IR analysis but FAME conversion was quantified from ^{1}H-NMR. In order to obtained maximum FAME conversion of 96.7%, process parameters were optimized as: catalyst concentration (1.5wt%), oil to alcohol molar ratio (1:14), stirrer speed (600 rpm), temperature (65˚C), and reaction time (40 min) in presence of co-solvent (DPE). Reusability of the catalyst was also investigated and it was found that up-to eight times the conversion efficiency was quite significant (more than 75%). The quality of synthesized biodiesel was compared as per ASTM biodiesel standard and it was found to be quite compatible with conventional diesel fuel.